The effects of steric hindrance on sub-glass transitions in epoxy polymers

Edward Balizer* and James V. Duffy
Naval Surface Warfare Center, Silver Spring, MD 20903-5000, USA
(Received 26 March 1991; accepted 16 April 1991)

Pairs of sterically hindered and unhindered linear aliphatic and aromatic diamines were synthesized and used as curatives for the diglycidyl ether of bisphenol A (DGEBA). The steric hindrance was caused by methyl group substitution of a hydrogen atom adjacent to the amine. For each pair, the hindered diamine cure had a lower density and a higher glass transition. Another pair of diamines was synthesized for which the methyl group was replaced by ethyl and butyl side chains; for these resins, both the density and glass transition decreased. Torsional pendulum results show that the sub-glass transition for the hindered cures shifts to lower temperatures and has a greater activation energy. Analysis by the Havriliak–Negami dispersion equation shows that the hindered resins have broader and more symmetrical relaxations. The background hysteresis loss outside of the relaxation region was analysed by the Nutting equation and was found to decrease with steric hindrance.

(Keywords: diglycidyl ether of bisphenol A; steric hindrance; diamines; sub-glass transition; Havriliak–Negami dispersion; hysteresis dispersion)

INTRODUCTION

The secondary or γ transition in DGEBA epoxies (diglycidyl ether of bisphenol A) has been studied as a function of cure and the amount and molecular structure of diamine hardeners[1–7]. Dynamic mechanical experiments by torsional pendulum show that the temperature of the transition and the activation energy are dependent on both diamine structure and extent of cure[5–7]. The mechanical response, the loss modulus G'' in particular, of the γ relaxation for a series of aliphatic diamines was uniquely dependent on varying methylene content and therefore not superimposable[7].

Recent torsional pendulum measurements[8] in our laboratory on the γ transition in DGEBA resin have extended the above studies to include the effects of steric hindrance in linear diamines. The unhindered and hindered diamine pair was silicone diamine (SiDA) and tetramethyl silicone diamine (TMSiDA) respectively. In TMSiDA, the carbon atom adjacent to the amine group was methylated and provided hindrance to bond rotation. The resulting γ transition for the TMSiDA cure (hindered) was lowered by 20°C relative to that of the SiDA (unhindered) at -50°C. The decrease in area of the loss curves also revealed a lower activation energy for the hindered diamine. To extend our investigation of steric hindrance in DGEBA resins, additional pairs of hindered and unhindered diamines were synthesized: a linear aliphatic pair, an aromatic pair and one with extended hydrocarbon side chains of ethyl and butyl in place of the methyl group. The dynamic moduli for the γ relaxation for each member of the pairs differed in relaxation temperature, activation energy and asymmetry.

In order to correlate all of these effects in our analysis, the dynamic modulus G' and loss G'' were fitted to the Havriliak–Negami equations[9], as they contain parameters for mechanical properties as well as for the shape dependence of the transition. We extended the analysis for the dynamic modulus beyond the relaxation region to include the background losses in the relaxed and unrelaxed temperature regions as shown in *Figure 1*. The energy loss per cycle in these regions has been found to be independent of frequency and to be a hysteresis loss by both mechanical and dielectric measurements[10,11]. An analytical expression for the complex dynamic modulus in these regions was determined from the Nutting equation[12], for which the loss tangent is frequency-independent and therefore compatible with a hysteresis loss. It is the purpose of this paper to analyse, by both the Havriliak–Negami (HN) and Nutting dispersion equations, the effects of steric hindrance on the γ transition as measured by torsional pendulum for the above DGEBA resins.

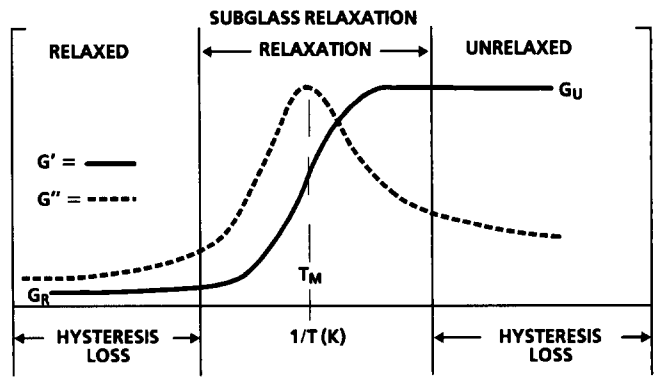

Figure 1 Sub-glass relaxation region (schematic)

* To whom correspondence should be addressed

0032-3861/92/102114-09

EXPERIMENTAL

Polymer synthesis

A number of pairs of hindered/unhindered diamines were used in this study as curatives for DGEBA. The diamines had the generalized structure (I) shown below:

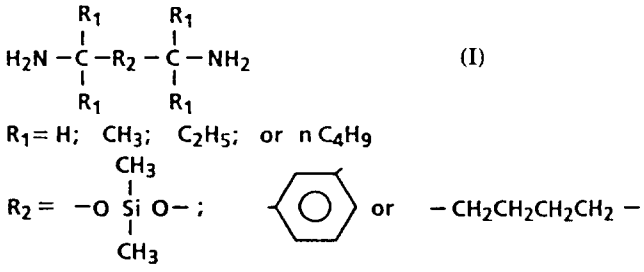

The two silicone-containing diamines were synthesized as follows:

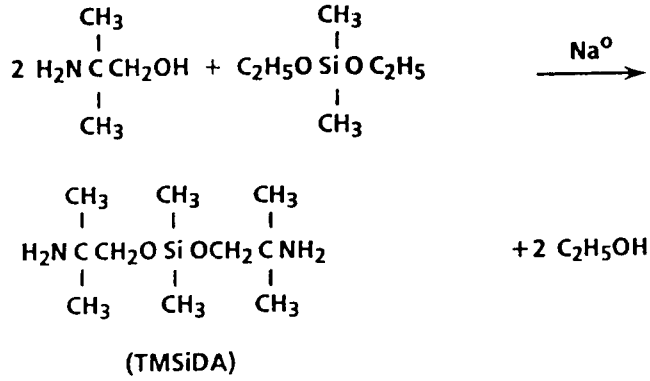

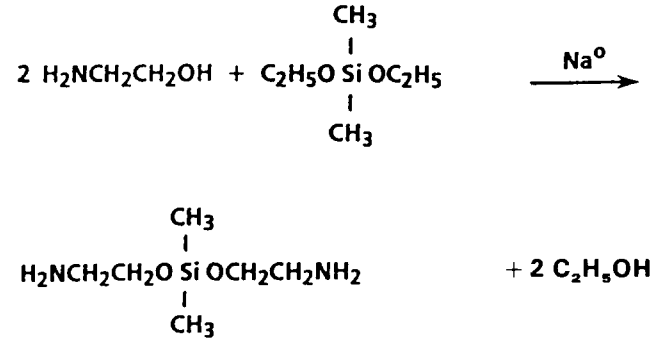

The amines bis(β-aminoethoxy)dimethylsilane (SiDA) and bis(β-amino-β-methylpropoxy)dimethylsilane (TMSiDA) were distilled and their purity was determined by gas chromatographic analysis, while structural verification was made by n.m.r.

In the case of the two aromatic amines used in this study, *m*-xylylenediamine (*m*XDA) was purchased from Aldrich Chemical Co., Milwaukee, Wisconsin, and was used without further purification. The hindered amine *m*-tetramethylxylylenediamine (*m*TMXDA) was supplied by American Cyanamid, Bound Brook, New Jersey, and was also used without further purification.

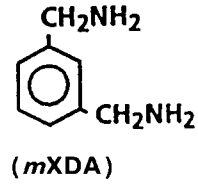

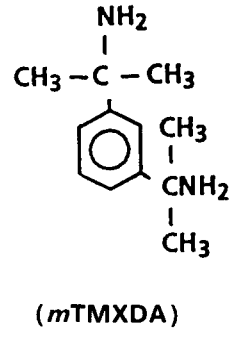

Three amines comprised the aliphatic series of hindered amines, which were derived from the unhindered parent amine 1,4-diaminobutane (BDA).

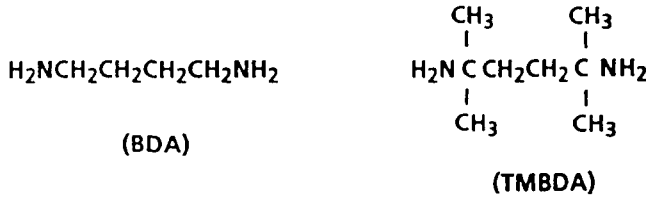

Both BDA and 2,5-dimethyl-2,5-diaminohexane (TMBDA) were purchased from Aldrich Chemical Co. and used without further purification. The 3,6-diethyl-3,6-diaminooctane (TEBDA) and 5,8-di-n-butyl-5,8-diaminododecane (TBBDA) were synthesized as follows:

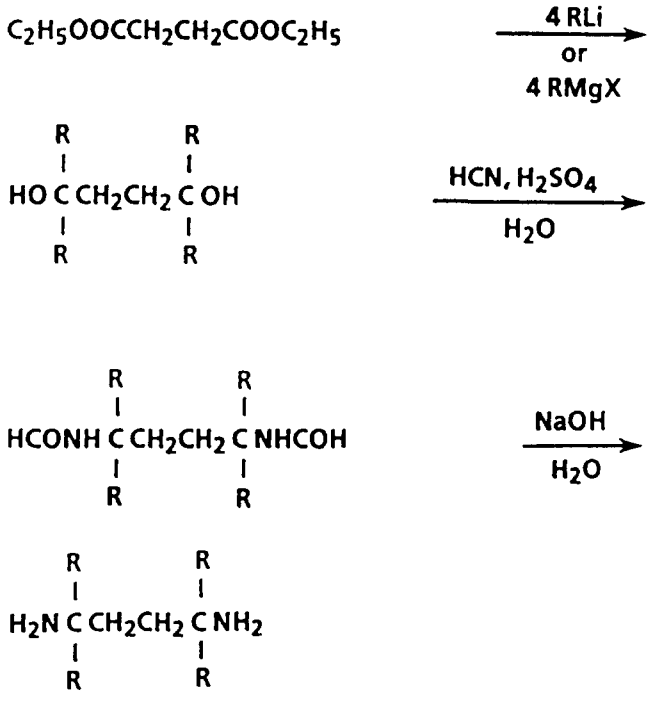

These amines were purified by distillation, and structural verification was accomplished by n.m.r., thin-layer chromatography, infra-red spectroscopy and elemental analysis.

The diglycidyl ether of bisphenol A (DGEBA) (II)

was purchased from the Dow Chemical Co., Midland, Michigan, and used as received. The generalized epoxy–amine reaction can be represented as follows:

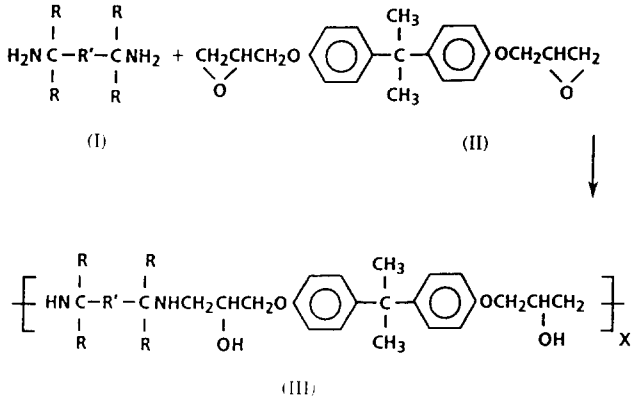

The intermediate reaction product (III) can further react through the secondary amine hydrogens and additional DGEBA to yield a highly crosslinked thermosetting epoxy resin.

Stoichiometric quantities of each amine were added to DGEBA and the mixture thoroughly mixed, poured into a mould and allowed to react at room temperature under nitrogen for a period of 2 days. The final cure cycle used was as follows: 50°C/2 h, 80°C/2 h, 100°C/24 h, 140°C/2 h and 160°C/2 h.

Density

Samples of nominal measurements of 63 mm by 12 mm by 3.1 mm were measured by immersion according to ASTM method D792.

Thermal analysis

The glass transitions of the resins were measured with a DuPont 9900 Thermal Analyzer in conjunction with a 910 differential scanning calorimeter (d.s.c.) module. The heating rate was 10°C min^{-1} and the sample was scanned from 0 to 150°C in an argon atmosphere.

Dynamic mechanical properties

Dynamic mechanical measurements were taken on a torsional pendulum after a design of Nielsen[13]. After manually exciting the torsional pendulum into free oscillations, the resulting damped waves were digitized and stored on a waveform recorder (Hewlett–Packard 7090A). The logarithmic decrement was calculated from the waveforms using the relationship:

$$\Delta = (1/n)\ln[A(r)/A(r+n)] \quad (1)$$

where $A(r)$ is the amplitude of a reference peak and $A(r+n)$ is the amplitude of a peak n cycles later.

The shear modulus (Pa) is calculated from the equation:

$$G = 0.235LI/CD^3\mu P^2 \quad (2)$$

where L is the length (cm) of the specimen between the clamps, C is the width (cm), D is the thickness (cm), I is the moment of inertia (g cm^2) of the oscillating system, μ is the shape factor and P is the period of oscillation. An automated computer system was used to obtain both logarithmic decrement and shear modulus as a function of temperature. A non-linear least-squares method was used to determine a six-parameter equation for the angular displacement data. The equation assumed to represent the digitized data is:

$$\Theta = \Theta_0 \exp(-\alpha t)\cos(\omega t - \phi) + Dt + B \quad (3)$$

where Θ_0 is the initial amplitude, α is the damping coefficient, ω is the angular frequency (rad s^{-1}), ϕ is the phase angle, D is the drift coefficient and B is the offset voltage. D is related to the drift in the output voltage of the linear differential transformer used in converting the mechanical motion of the pendulum to an electric signal. B is the charging voltage, approximately 7–8 V across the linear voltage differential transformer. In this case the loss per cycle is found as:

$$\Delta = \alpha P \quad (4)$$

where $P = 2\pi\omega$. The loss shear modulus is then calculated as:

$$G'' = G'\Delta/2\pi \quad (5)$$

Samples of nominal area of 63 mm × 12 mm and three thicknesses of 0.56 mm, 1.08 mm and 3.1 mm were cast to cover the temperature range of −180 to 180°C for torsional pendulum measurements. The thickest sample was measured from the glass transition to the rubbery state, the thinnest from ambient to −180°C and the remaining sample from ambient into the glass transition. The rate of change of temperature was approximately 0.17°C min^{-1}.

THEORY

The Havriliak–Negami relaxation equation

The relaxation of the shear modulus can be mathematically represented equivalently as a function of time or of frequency. This approach developed for a single relaxation time for dielectric relaxations by Debye[14] has been extended by Havriliak and Negami to a distribution of relaxation times and to include mechanical dispersions.

The frequency representation for the complex modulus as found by Havriliak and Negami[9] (HN equation) is:

$$G^* = G_U - (G_U - G_R)/[1 + i(\omega\tau)^A]^B \quad (6)$$

where G_U and G_R are the unrelaxed and relaxed moduli, ω is the excitation frequency and τ is the average relaxation time. The parameter A ($0 < A < 1$) broadens the width of the relaxation as it decreases in value; the parameter B ($0 < B < 1$) causes a skewing or asymmetry in the modulus in both real and imaginary parts as a function of frequency.

The temperature dependence of the HN equation is introduced by assuming an Arrhenius behaviour for the relaxation time τ as follows:

$$\tau = \tau_0 e^{-H/RT} \quad (7)$$

where τ_0 is a fundamental relaxation time occurring in the limit of high temperature, H is a barrier energy between transition states, R is the gas constant (1.98 cal mol^{-1}) and T is the kelvin temperature. It is well documented that relaxation times in the glassy state are of this temperature dependence[15]. In order to better represent experimental data, each of the parameters of the HN equation is assumed to behave linearly in

temperature in the relaxation region. Thus we have:

$$\begin{aligned} G_U(T) &= G_U(T_m) + G'_U(T - T_m) \\ G_R(T) &= G_R(T_m) + G'_R(T - T_m) \\ A(T) &= A(T_m) + A'(T - T_m) \\ B(T) &= B(T_m) + B'(T - T_m) \end{aligned} \quad (8)$$

where T_m is a temperature in the relaxation region and is conveniently chosen as the peak of the loss modulus G'' so that several polymer cures can be compared. Although there is evidence that A and B show curvature with temperature[9], they can be approximated as linear over a limited temperature region and lead to reasonable results.

The peak temperature T_m of the loss modulus is determined from its temperature derivative, which yields, using the previous equations, an equation of the form:

$$\omega\tau_{max} = F(A(T), B(T), G_U(T), G_R(T), H, \tau_0) \quad (9)$$

where τ_{max} is the relaxation time at the G'' peak and the parameters in the function F have already been determined by fitting experimental data. Thus the reciprocal relationship between ω and τ_{max} for the Debye model is scaled by the function F, which may differ from unity by one or as much as two orders of magnitude when calculating ω from τ_{max} from the temperature-dependent HN dispersion.

The Nutting or hysteresis dispersion

When a relaxation is measured by either dielectric or mechanical spectroscopy, a background loss is present. The background energy lost per cycle is a constant or frequency-independent and is the hysteresis loss. As will be shown for our results, the inclusion of a hysteresis loss can account for otherwise anomalous behaviour when fitting experimental data with just the HN dispersion.

We derive the frequency-dependent hysteresis dispersion for the complex modulus from the relaxation given by the Nutting equation below:

$$G = G_0 t^{-v} \quad (10)$$

where G_0 is a constant and the constant v is small compared to unity. The frequency dispersion obtained from the relaxation time spectral density of the above power law by Alfrey's rule[16] is $G_0 v\tau^{-v}$. The standard viscoelastic transformation equations of the spectral density $H(\tau)$[17] yield the complex modulus as shown below:

$$G' = G_0\omega^v \quad (11)$$

$$G'' = \pi v G_0 \omega^v/2 \quad (12)$$

where approximation was made for small v. It is evident that the loss tangent is:

$$\tan\delta = G''/G' = \pi v/2 \quad (13)$$

which yields that the loss per cycle is frequency-independent. It is important to note that the spectral density contains the factor v and not just a constant. For, as the energy dissipated per cycle approaches zero, indicating a perfectly elastic material, the density and the imaginary part of the modulus approach zero; however, the real shear modulus approaches the constant G_0.

RESULTS

The fitting

The resulting data, as shown in *Figures 2a* and *2b*, of the modulus G' and loss modulus G'' for BDA and TMBDA over the temperature range of -180 to 20°C show the sub-glass relaxation at -70°C. Also included in this and each subsequent figure are fitted curves corresponding to the HN and hysteresis dispersions. Similar data were taken and fits made for *m*XDA and *m*TMXDA (*Figures 3a* and *3b*), SiDA and TMSiDA (*Figures 4a* and *4b*) and the series of side-chain-substituted BDA of TEBDA and TBBDA (*Figures 5a* and *5b*). The data in the relaxed region bordered on the glass transition and were therefore truncated so as not to include its effect. The corresponding G'' values show a peak at the γ relaxation.

The quantity G'' rather than $\tan\delta$ was considered a more fundamental quantity, which could be directly fitted to the Havriliak–Negami equations. As the HN parameters occur in the complex modulus, both G' and G'' were simultaneously fitted to the data. Initially, we used temperature-independent parameters for the constants G_U, G_R, A and B and minimized the difference between fitted and experimental data (residuals). The

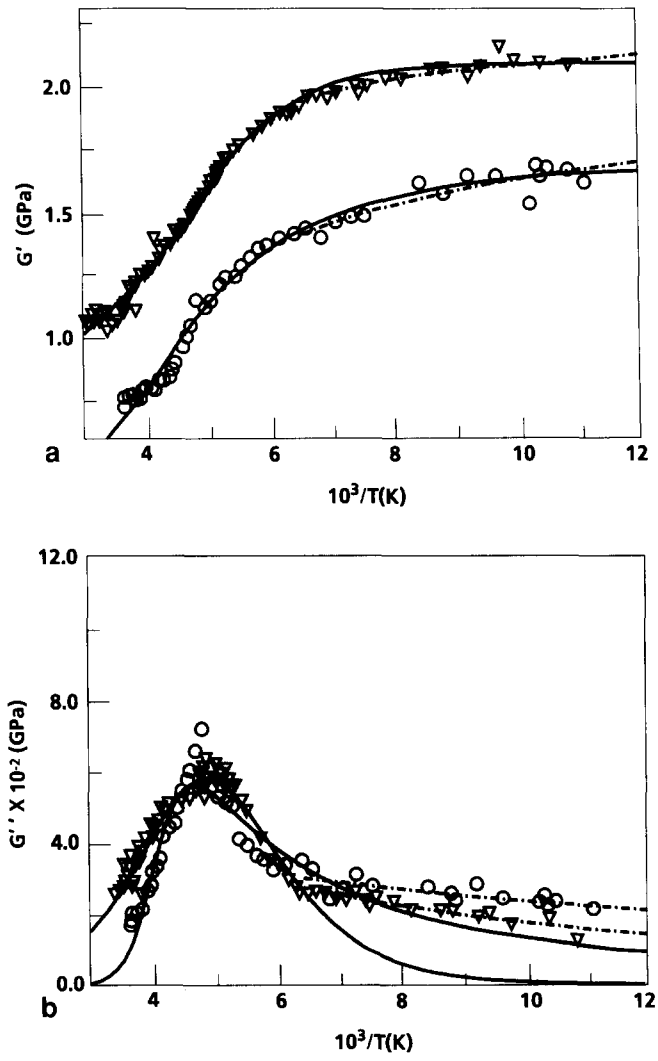

Figure 2 Sub-glass relaxation region: (○) BDA, (▽) TMBDA; HN dispersion (——), hysteresis dispersion (—·—); (a) shear modulus, (b) loss modulus

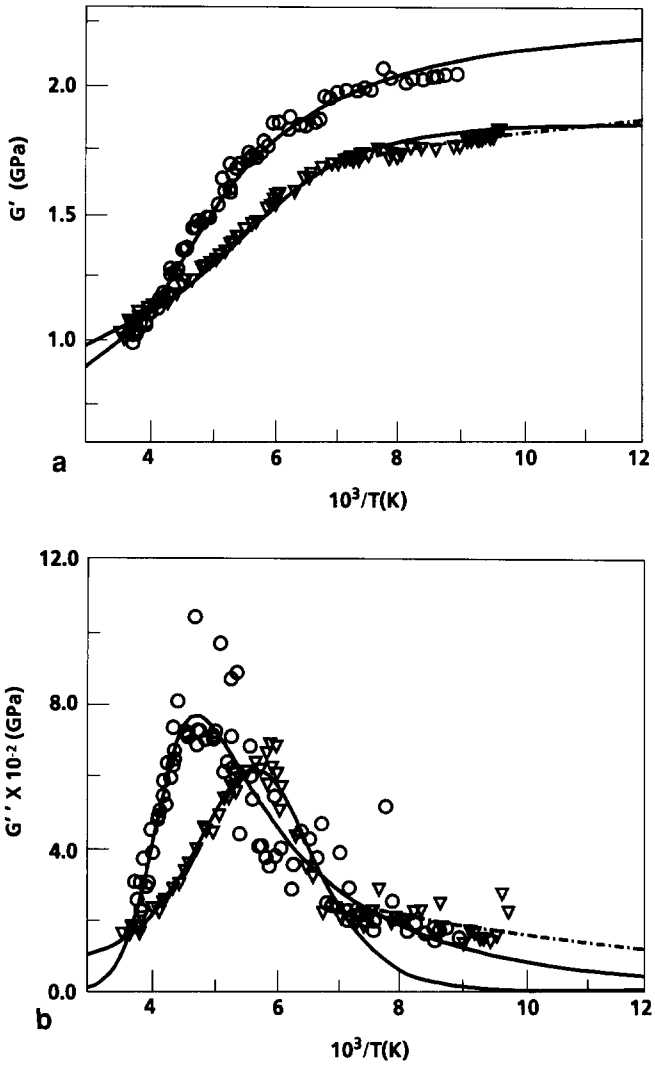

Figure 3 Sub-glass relaxation region: (○) *m*XDA, (▽) *m*TMXDA; HN dispersion (——), hysteresis dispersion (—·—); (a) shear modulus, (b) loss modulus

resulting fit to G' was very good, while that for G'' was poor in determining the value of the temperature and shape of the maximum of the relaxation peak. However, when weighting the residuals to account for the difference in magnitude between G' and G'', the G'' fit improved at the expense of that of G'; either G' or G'' could be fitted but not both simultaneously.

When allowing linear temperature dependences for the relaxed and unrelaxed moduli, G_U and G_R and the width parameter A, very good fits for both G' and much of G'' over the temperature range of the relaxation resulted, as shown in *Figures 2–5*. In the unrelaxed region between -120 and -180°C the experimental values of G'' were always greater than the analytical fit for each of the epoxy cures. The large asymmetry required to fit the data in this temperature region yielded very small values of B and the fit was still in doubt. Allowing the B parameter to be linearly temperature-dependent produced anomalies in the shear modulus G': it peaked and decreased with decreasing temperature. As the temperature-independent fits of B did not show anomalies and yielded as good fits as those with temperature dependence, we proceeded by keeping it a constant. Care has to be taken in the assumption of linearity on temperature for the HN fitting parameters, as extrapolating the HN equations beyond the temperature range of fit can result in anomalous behaviour in both G' and G''.

The lack of fit of the G'' data, always by underestimation, indicated to us that another loss process occurred at temperatures below -120°C. We were then motivated to include a hysteresis loss in this low-temperature region. Including this loss necessitates defining an upper and lower bound of temperatures for which the γ relaxation dominates the hysteresis loss. The transition between the hysteresis loss and relaxation was determined by incrementing the temperature towards lower values in the unrelaxed region to fit the G'' loss peak to the HN equation. This process was continued until the calculated G'' deviated from the contour of the experimental G'' loss peak. This last temperature, the cut-off temperature, was then used as the lower bound for the HN fit. This temperature varied from cure to cure but was consistently in the range of -120 to -130°C for the aliphatic and somewhat lower for the aromatic backbones. The upper bound for the relaxation was chosen close to room temperature (20°C) as for temperatures greater than this the glass transition as well as some secondary pre-glass transitions were evident in the spectra. The resulting parameters of the best HN fit were then used in an analytic expression for the derivative of

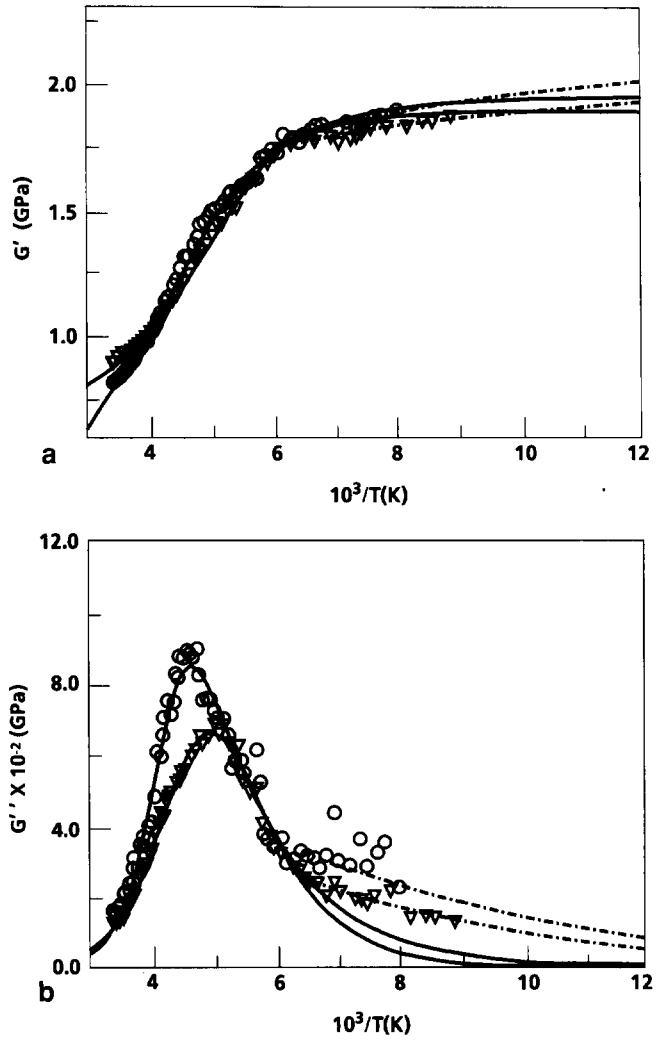

Figure 4 Sub-glass relaxation region: (○) SiDA, (▽) TMSiDA; HN dispersion (——), hysteresis dispersion (—·—); (a) shear modulus, (b) loss modulus

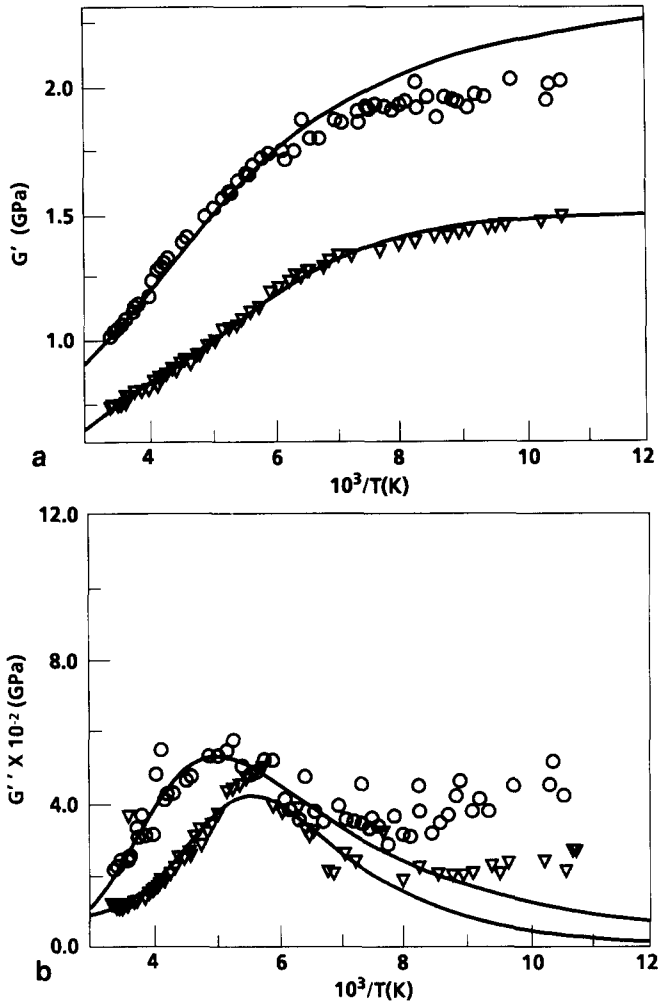

Figure 5 Sub-glass relaxation region: (○) TEBDA, (▽) TBBDA; HN dispersion (——), hysteresis dispersion (—·—); (a) shear modulus, (b) loss modulus

Table 1 Characterization of cures

Hardener	T_m (K)	T_g (K)	Density (g cm^{-3})
SiDA	215	350	1.1833
TMSiDA	201	355	1.1575
BDA	213	386	1.1794
TMBDA	204	409	1.1512
TEBDA	197	402	1.1408
TBBDA	178	391	1.0963
*m*XDA	210	389	1.1881
*m*TMXDA	179	422	1.1587

G'' to determine the temperature of the relaxation peak, T_m.

The G'' data for the temperature region below the lower cut-off was attributed exclusively to hysteresis. In this temperature region, both the shear modulus and loss modulus were simultaneously fitted to the frequency representation of the Nutting equation of the previous section. Again, both parts of the modulus were simultaneously fitted and the residuals of the lossy part weighted. A linear temperature dependence for both the modulus and exponential were assumed. The experimental data were now well fitted to the hysteresis moduli with a much improved fit for G''. Owing to the difficulty in establishing the overlap region where both relaxation and hysteresis losses occur, we have made the approximation that the cut-off is sharp and only one loss mechanism occurs: either relaxation or hysteresis. This leads to non-continuous functions of temperature as noticed in the figures for each of the cures. The continuity of the functions G' and G'' can be implemented but would require additional parameters for the Nutting equation.

Results of measurements and fits

We now present the values of the measured densities and the results of the d.s.c. scans in order to relate them to the parameters of the HN fits. The densities and d.s.c. T_g values are listed in *Table 1* as well as values for T_m for comparison. The four pairs of hindered and unhindered diamine epoxies show similar trends. For each pair, the methylated diamine has a lower density and a higher T_g. The greater interchain steric hindrance of the methyl groups creates a greater volume for these resins and reduces the density. However, the intrachain steric interactions cause a stiffening of chains that increases the glass transition[18]. For the family of BDA cures, increasing the length of the side chain decreases the density and decreases the glass transition. It appears that the butyl group does not sterically hinder intrachain motion as does the methyl group. Thus for TBBDA, with the longest alkyl side chain, the T_g at 118°C is closest to that of the unhindered BDA at 113°C. The direct steric hindrance of the methyl group to the backbone is responsible for the trend of T_g.

The HN dispersion

The HN parameters for the γ relaxation for each cure are listed in *Table 2*. In order to compare the relaxation in the hindered and unhindered cure pairs, the temperature-dependent parameters are evaluated at T_m, the temperature for which G'' has a maximum. As shown

Table 2 HN relaxation parameters for γ relaxation

	G_U (GPa)		G_R (GPa)		A		
Hardener	$G_U(T_m)$	G'_U	$G_R(T_m)$	$G'_R \times 10^3$	$A(T_m)$	A'	$B(T_m)$
SiDA	1.95	$-1.01(10^{-6})$	1.08	−3.74	0.537	$-1.67(10^{-4})$	0.195
TMSiDA	1.90	$-5.24(10^{-10})$	0.98	−1.33	0.200	$4.89(10^{-3})$	0.784
BDA	2.33	$-5.75(10^{-6})$	0.87	−3.24	0.448	$2.57(10^{-3})$	0.098
TMBDA	2.09	$-1.88(10^{-6})$	1.14	−1.42	0.185	$-6.06(10^{-6})$	0.630
TEBDA	2.38	$-7.74(10^{-7})$	1.14	−1.92	0.183	$4.77(10^{-4})$	0.317
TBBDA	1.51	$-9.47(10^{-9})$	0.90	−1.78	0.454	$-7.71(10^{-4})$	0.259
*m*XDA	2.24	$-7.23(10^{-7})$	1.13	−1.85	0.418	$9.05(10^{-4})$	0.170
*m*TMXDA	1.85	$-1.15(10^{-7})$	1.13	−1.10	0.280	$-6.83(10^{-5})$	0.451

Table 3 Parameters for relaxation times

Hardener	τ_0 (s)	H (kcal mol^{-1})	T_m (K)	Temp. range (K)
SiDA	$1.23(10^{-11})$	11.7	215	153–292
TMSiDA	$1.38(10^{-19})$	17.4	201	153–294
BDA	$2.94(10^{-12})$	12.4	213	153–273
TMBDA	$3.60(10^{-17})$	16.0	204	147–293
TEBDA	$5.40(10^{-15})$	14.2	197	153–292
TBBDA	$6.50(10^{-12})$	10.5	178	113–291
*m*XDA	$3.90(10^{-14})$	14.2	210	93–264
*m*TMXDA	$3.40(10^{-15})$	11.7	179	133–279

above, methyl group hindrance increases the T_g in order of rigidity of backbone TMSiDA, TMBDA, *m*TMXDA. The corresponding sub-glass transition temperatures T_m, however, decrease by 10–15°C for cures of hindered backbones (*Table 3*). The aromatic *m*TMXDA has an even greater downward shift of 30°C when compared to the unhindered *m*XDA. The decrease in T_m for the hindered cures occurs as their lower density creates a greater volume for the local relaxational motion. Although the temperatures T_m decrease, their corresponding activation energy H increases. This is an unexpected result, as one would expect a greater activation energy at higher temperatures. Unlike the aliphatic cures, the aromatic amine cures have the lowest transition temperature coinciding with the lowest activation energy, which is the expected trend. Although the *m*TMXDA density is similar to those of the other hindered amine cures, it has the largest decrease in density of all the cures relative to its unhindered counterpart, which may affect its transition temperatures accordingly.

The series of BDA, TMBDA, TBBDA and TEBDA shows that the effect of adding longer side chains lessens the steric interaction of the appending methyl group with the backbone chain. Both the sub-glass and glass transition temperatures for this group of cures decrease as does their density. Thus the molecular motion is highly dependent on volume. The side chains add end defects, which lower T_g, and if they contain three bonds can contribute to another pre-glass relaxation[19]. The G'' data for TEBDA and TBBDA had scatter about the γ relaxation, which added difficulty in determining whether an additional relaxation occurred in the side chain, in particular for TBBDA. Note the γ transition peak for the BDA cures shows no indication of levelling off, which indicates the possibility of another loss.

The shape of the relaxation curves *versus* temperature are strongly affected by steric hindrance, as noted upon comparing the curves for the methylated and unmethylated cures. For each pair of cures the hindered group extends the G'' relaxation to higher temperatures. These curves are therefore broader and hence have smaller A values (see *Table 2*) than the unhindered cure. This is expected as the hindered cure requires a higher temperature for local modes to become active while at lower temperatures its greater volume enables motion to occur. As the relaxations contributing to G'' extend into the lower temperature regions for the hindered cures, larger B parameters were obtained, indicating a greater symmetry for the relaxation of these cures.

The strength of the relaxation or the maximum value of G'' for the Debye single-relaxation-time model is proportional to the difference between the relaxed and the unrelaxed modulus. The HN model yields a more complicated expression for the maxima, especially when the temperature dependence of parameters is included. As a result, the shear modulus in the unrelaxed and relaxed regions may not be extrapolated beyond the range of the relaxation as can be done for the Debye model. Thus, to compare trends of relaxation strength, the moduli were evaluated at the G'' peak temperature T_m. The unrelaxed modulus is approximately double that of the relaxed moduli, which is usual for a sub-glass transition. For all the cures, the unrelaxed modulus of the glassy state for the unhindered cure is greater than that of the hindered cure. This is reasonable, as there are less polymer chains per cross-sectional area as corresponds to the respective densities of the cures. This result we find applicable only when comparing cures of hindered and unhindered pairs but not when comparing all the cures on the basis of density alone. This indicates that other interactions have to be considered for discussion of G_U in general. Assuming that the relative values of the specific volumes found at room temperature can be extrapolated to lower temperatures of the unrelaxed region, we find that the change in the modulus $G_U(T_m)$ between hindered and unhindered cure pairs follows their density difference. This is illustrated by the data for the *m*TMXDA and *m*XDA pair, which have the largest relative difference in density and $G_U(T_m)$. We find the same trends for $G_U(T_m)$ for the BDA group with increasing side-chain length. The relaxed moduli $G_R(T_m)$ values are closer in value for both hindered and unhindered cures. However, in the relaxed region beyond the peak in G'', the unrelaxed moduli of the hindered group are slightly greater due to both viscosity and rotational hindrance of the methyl group.

The hysteresis dispersion

The data for the cures were fitted with the Nutting equation in the unrelaxed regions that were defined by the cut-off temperatures determined by the HN fit. The hysteresis moduli were plotted for the fitted temperature region below the cut-off temperature; the HN results were extrapolated beyond their fitted region into the hysteresis region for comparison. Linear temperature dependences for the modulus G_U and the energy loss per cycle v were assumed. These values appear in *Table 4* and are referenced to a temperature of −160°C, which we feel is out of the relaxation range. The experimental values of the torsional pendulum frequencies also appear and are used in the Nutting equation. The trends in the unrelaxed modulus G_U parallel those that were found in the relaxation region for the HN dispersion. The losses varied with aliphatic and aromatic backbones as well as

Table 4 Nutting equation parameters

	G_U (GPa)		v		
Hardener	$G_U(113)$	$-G'_U$	$v(113)$	$v' \times 10^4$	f (Hz)
SiDA	1.89	3.49	6.49	1.26	1.69
TMSiDA	1.84	2.59	4.89	1.02	1.12
BDA	1.53	4.26	10.50	0.08	1.35
TMBDA	2.02	2.75	6.41	0.07	1.11
*m*XDA	–	–	–	–	–
*m*TMXDA	1.75	3.27	6.82	0.93	1.22

with hindrance and non-hindrance. The energy dissipated due to the hysteresis mechanism appears greater for the non-hindered cures. The aromatics have a small contribution or none at all to the hysteresis mechanism as illustrated in *Figure 3b* for *m*XDA and *m*TMXDA. Unfortunately, there was more scatter in this lower-temperature region for the BDA cure and its group with extended side chains, so the hysteresis loss was not amenable to analysis. The greater loss for the unhindered linear diamine cures does not follow a dependence where greater volume due to structural hindrance yields a greater loss. This of course assumes that the densities at these temperatures follow those at room temperature.

The hysteresis is expected to be volume-dependent; the less the volume, the lower the loss, until a cut-off volume is obtained for which the loss cuts off. We find that the volume increase induced by the structure of the hindered cures has a smaller hysteresis than unhindered cures of smaller volume. However, the loss accompanying thermal expansion as noted by the thermal coefficient of v increases with temperature. Thus a general change in volume can affect the loss differently and depends how the volume is created: thermally or structurally.

DISCUSSION

Hysteresis dispersion

Using our dispersion relations for the hysteresis moduli we can compare our data to a homologous series of epoxies of linear aliphatic diamines of three, six and 10 carbon atoms and our BDA cure of four carbon atoms. The measurements of the homologous series of epoxies were made at 2 MHz at 20°C[20] and are in the glassy state. The frequency dispersion and constant value of v allow both G and its temperature derivative to be easily shifted to 1 Hz from 2 MHz. Our experimental value for the shear modulus for BDA of 0.7 GPa at 20°C fits very well within the series, as does as its temperature derivative as determined from room-temperature data. These results using the Nutting frequency dispersion well substantiate a hysteresis mechanism at this temperature. When using the v parameter from data fitted below −120°C, therefore below the sub-glass transition, and extrapolating to 20°C, the v values (losses per cycle) were about half that of the room-temperature ultrasonic values. The assumption that the loss per cycle is linear in temperature over such a large temperature range and especially through a transition is doubtful. This indicates that the loss decreases non-linearly over the entire temperature range and more slowly at temperatures below that of the γ relaxation.

The source of the hysteresis loss appears to be due to non-linear processes. Data in the literature for two series of epoxies of diglycidyl ether of bisphenol A and resorcinol diglycidyl ether cured with the same diamines show that the ultrasonically measured loss is greater for cures of greater thermal expansion[20]. As the thermal expansion depends on higher order than harmonic terms for a potential, this indicates that a non-linear interaction may also be responsible for the hysteresis loss. From our results above it seems that the stiffer chains possessing aromatic backbone groups or side groups hindering the backbone have the smallest loss per cycle. This motional hindrance would prevent large displacements that would lead to non-linear effects such as hopping between metastable minima and reduce the hysteresis loss.

The HN parameters and cure

The values of the activation energy H from the HN analysis are in the range of 11 to 20 kcal mol^{-1} for the hindered and unhindered diamines. These values are at the lower range of activation energies as reported by Arridge[6] for DGEBA/EDA (ethylenediamine) cures. His values of the activation energy are highly cure-dependent and vary sigmoidally from 14 to 26 kcal mol^{-1} as the network is cured from about 70% to a cure approaching 95%. The activation energies for maximum cure are greater than ours but Arridge calculated the energies by the method of Read and Williams[21] from the area under the G'' curve with respect to the reciprocal temperature.

Arridge proposed the ratio of the modulus at 20°C to that at −196°C as a figure of merit for degree of cure of DGEBA/EDA, the value of which ranged from 0.42 or less for a highly cured network to 0.50 or greater for a 70% cured network. A similar ratio of the modulus at −162°C to 20°C for our series of cures yielded 0.244 for the unhindered amine cures and 0.53 for the hindered amine cures. We believe the difference in value to be due to steric hindrance of the shear modulus and not extent of cure. The ratios for the non-hindered systems are in agreement with the low values of the activation energies and appear to indicate that the cure has not reached saturation.

Comparison to models of local motion

We interpret the trends of our results qualitatively by two local-mode theories for the glassy state. One is an equilibrium model of Hayakawa and Wada[22], which relates the relaxation strength and the unrelaxed and relaxed moduli; the other is a time-dependent or dispersion model of Mansfield[23]. Hayakawa and Wada's model consists of bond rotations interacting with a nearest-neighbour torsional constant f and an intermolecular torsion constant g, which is a function of interchain distance and is sensitive to displacements. For our cures, the steric interaction of the methyl groups increases the intermolecular distance and decreases the dispersion forces; thus decreasing the value of g. Concurrently the number of active sites per unit volume would also decrease with the methylation as the density is decreased. The strength of the relaxation at the same temperature would tend therefore to be weaker, according to Wada's theory, for the sterically hindered cures. This is certainly apparent when comparing the heights of the G'' for each of our pairs of hindered and unhindered cures in each of the figures.

Hayakawa and Wada's model is an equilibrium theory and therefore unable to consider the time dependence of the relaxation. A recent analytical model for local-mode relaxations was presented by Mansfield, in which he found the time correlation function for the angular motion and related his solution specifically to the HN expression. However, the data generated by Mansfield were for the value of the intramolecular coefficient much greater than the solvent (intermolecular) interaction and not applicable to our epoxies.

The localization of molecular motion

The molecular motion that is responsible for the γ peak in epoxy cures has been localized to the glycidyl group produced during crosslinking. In this section we wish to discuss the localization of the motion in the epoxy cures

by comparing data from dynamic mechanical results along with those from thermally stimulated depolarization (t.s.d.) and n.m.r. experiments. Torsional pendulum experiments on DGEBA cures with no added diamines and therefore no glycidyl groups yielded a sub-glass transition temperature at $-70°C$[24]. As diamines and therefore glycidyl groups were introduced incrementally into the cure, the peak of the transition broadened and shifted to higher temperatures. Upon blocking the motion of the glycidyl groups, the relaxation for the diamine cures reproduced that of just the ether cure. These results indicated that the relaxation was attributed to two processes where motion occurred over both ether and glycidyl linkages. Similar sub-glass relaxations were determined over a broad series of epoxy diamine cures by t.s.d.[25], which has an effective frequency of 1/1000 Hz and was able to detect two sub-glass transition peaks. The higher-temperature peak would correspond well to the glycidyl motion while the lower-temperature peak corresponds to motion of the ether group, as only charged groups could be measured in this experiment. For the DGEBA cure, these peaks overlapped such that the t.s.d. spectra consisted of a single broad peak with a shoulder. If measured at a higher frequency by dynamic mechanical experiments, the overlap would be more severe and a single peak would result. We surmise that the molecular motion of the sub-glass transition in our cures may be more delocalized than a crankshaft of the glycidyl group.

CONCLUSIONS

The inclusion of steric hindrance in DGEBA resins decreases their density and intermolecular interactions. The complex modulus analysed in the relaxation region by the HN equation reveals that hindrance lowers the transition temperature and raises the activation energy. The increase in volume broadens the relaxation to the lower and the stiffness to the higher temperature regions. This tends to induce a more symmetric relaxation. The molecular motion responsible for the transition may not be localized only in the glycidyl groups, as other spectroscopies indicate that ether linkages may contribute to mechanical measurements for DGEBA resins. The background modulus for regions bordering the relaxation indicate a hysteresis loss according to the Nutting equation. Although greater volume is available for the hindered cures, their energy loss per cycle in the unrelaxed region is less than those for the unhindered cures, indicating that stiffening of the backbone decreases hysteresis losses.

ACKNOWLEDGEMENTS

This work was sponsored by the Center's Independent Research Program. We acknowledge Gilbert Lee of this Center for his contribution of the SiDA and TMSiDA data and his assistance with the experimental measurements. The Electrosynthesis Company Inc. of East Amherst, New York, is acknowledged for the synthesis of several of the hindered amines used in this work.

REFERENCES

1 Cuddihy, E. F. and Moacanin, J. *J. Polym. Sci. (A-2)* 1970, **8**, 1627
2 Cuddihy, E. F. and Moacanin, J. 'Dynamical Properties of Epoxide: Transition Mechanism', *Adv. Chem. Ser.* 92, American Chemical Society, Washington, DC, 1970, Ch. 9
3 Pogany, G. A. *Polymer* 1970, **22**, 66
4 Pogany, G. A. *J. Mater. Sci.* 1969, **4**, 405
5 Arridge, R. G. C. and Speake, J. H. *Polymer* 1972, **13**, 443
6 Arridge, R. G. C. and Speake, J. H. *Polymer* 1972, **13**, 450
7 Charlesworth, J. M. *Polym. Eng. Sci.* 1988, **28**, 221
8 Duffy, J. V. and Lee, G. F. *J. Appl. Polym. Sci.* 1988, **35**, 1367
9 Havriliak, S. and Negami, S. *Polymer* 1967, **8**, 161
10 Hartmann, B. and Jarzynski, J. *J. Appl. Phys.* 1972, **43**, 4304
11 Chung, S. H., Pathmanathan, K. and Johari, G. P. *J. Polym. Sci. (B)* 1986, **24**, 2655
12 Nutting, P. *Proc. Am. Soc. Test. Mater.* 1921, **XXI**, 1162
13 Nielsen, L. E. *SPE J.* 1960, **16**, 525
14 Debye, P. 'Polar Molecules', Dover, New York, 1945
15 McCrum, N. G., Read, B. E. and Williams, G. 'Anelastic and Dielectric Effects in Polymeric Solids', Wiley, London, 1967
16 Alfrey, T. and Doty, P. *J. Appl. Phys.* 1945, **16**, 700
17 Ferry, J. D. 'Viscoelastic Properties of Polymers', 3rd Edn., Wiley, New York, 1980, Ch. 3
18 Gibbs, J. H. and DiMarzio, E. A. *J. Chem. Phys.* 1958, **28**, 373
19 Hiltner, A. and Baer, E. *Polymer* 1974, **15**, 805
20 Hartmann, B. and Lee, G. *J. Polym. Sci., Polym. Phys. Edn.* 1982, **20**, 1269
21 Read, B. E. and Williams, G. *Trans. Faraday Soc.* 1961, **57**, 1979
22 Hayakawa, R. and Wada, Y. *J. Polym. Sci., Polym. Phys. Edn.* 1974, **12**, 2119
23 Mansfield, M. L. *J. Polym. Sci., Polym. Phys. Edn.* 1983, **21**, 787
24 Ochi, M., Okazaki, M. and Shimbo, M. *J. Polym. Sci., Polym. Phys. Edn.* 1982, **20**, 689
25 Chang, T. D., Carr, S. H. and Brittain, J. O. *Polym. Eng. Sci.* 1982, **22**, 1205